

Influence of Sr doping on twin-wall structure and flux pinning of $\text{YBa}_2\text{Cu}_3\text{O}_{7-\delta}$ single crystals

K. Saito* and H.-U. Nissen

Laboratorium für Festkörperphysik, Eidgenössische Technische Hochschule (ETH), 8093 Zürich, Switzerland

C. Beeli

Ecole Polytechnique Fédérale de Lausanne (EPFL), CIME, 1015 Lausanne, Switzerland

T. Wolf, W. Schauer, and H. Küpfer

Forschungszentrum Karlsruhe, Institut für Technische Physik, Postfach 3640, D-76021 Karlsruhe, Germany

(Received 2 September 1997; revised manuscript received 18 May 1998)

The twin textures of two differently synthesized types of $\text{YBa}_2\text{Cu}_3\text{O}_{7-\delta}$ single crystals, differing strongly in their critical current density (j_c) levels, have been investigated by high-resolution transmission electron microscopy. One type of crystal which has higher j_c values and contains 1 at. % Sr shows twin lamellae with boundaries decorated by many small local strain fields. It is suggested that this twin boundary structure is due to Sr doping. The Sr clusters present in the lattice are assumed to enhance flux pinning, and thus to result in the higher j_c values observed. [S0163-1829(98)03734-5]

In a number of experimental studies, a substantial enhancement of the flux pinning effect in $\text{YBa}_2\text{Cu}_3\text{O}_{7-\delta}$ by the boundaries of polysynthetic twin lamellae has been demonstrated. (For an introduction, see Refs. 1–3). In spite of this, a controversy still exists as to whether the existence of twin boundaries is the crucial condition for effective flux pinning [which is then a main cause for high critical current density (j_c) values] in these $\text{YBa}_2\text{Cu}_3\text{O}_{7-\delta}$ single crystals. Since the early stages of research in this field, there have been a number of observations⁴ that can be taken as evidence that doping with certain transition-metal elements could have a significant effect on the internal microstructures of the crystals, including their twin textures. The present authors have previously investigated the size distributions of twin lamellae of $\text{YBa}_2\text{Cu}_3\text{O}_{7-\delta}$ single crystals as well as of their Sr-doped analogues,⁵ and it was found, for instance, that doping with 1 at. % of Sr resulted in finer lamellae and in a more regular size distribution of the twin domains. Several previous high-resolution transmission electron microscopy (HRTEM) studies of twin boundaries of $\text{YBa}_2\text{Cu}_3\text{O}_{7-\delta}$ single crystals have indicated variations in the nature of the twin boundary interface in $\text{YBa}_2\text{Cu}_3\text{O}_{7-\delta}$ crystals and their doped analogues.^{6–8} Zhu *et al.* presented evidence by HRTEM observations that incoherent twin boundaries, which involved not only a 180° rotation of the lattice across the boundary but also a translation along that boundary, actually occurred in fully oxidized $\text{YBa}_2(\text{Cu}_{0.98}\text{Zn}_{0.02})_3\text{O}_{7-\delta}$ crystals^{6,7} as well as in very pure (fully oxidized) $\text{YBa}_2\text{Cu}_3\text{O}_{7-\delta}$.⁸ Thus, a variability in the twin boundary interface can be assumed to be an intrinsic property of $\text{YBa}_2\text{Cu}_3\text{O}_{7-\delta}$ crystals. Consequently, different pinning properties of the twin boundaries may result from variations of the twin boundary structure.³ However, the details of the possible effects of local twin boundary structure on the critical current density are not yet fully understood. The present HRTEM observations of twin textures were therefore made on two different types of $\text{YBa}_2\text{Cu}_3\text{O}_{7-\delta}$ single crystals having a large difference in their level of critical current densities.^{3,5} The aim of this study was to find any

variation in the nature of the defect structure between these two types of crystals that could explain the differences in the j_c values.

The fabrication processes for the two different types of crystals of $\text{YBa}_2\text{Cu}_3\text{O}_{7-\delta}$ were very similar and these crystals resembled each other in some of their physical and microstructural properties. The pertinent data on the synthesis as well as the previously measured physical properties³ of both types of samples (designated batch *A* and *B*) are listed in Table I. The batch *A* crystals with low j_c values were grown from a mixture of 4N purity chemicals, and they were then quenched, while the batch *B* crystals were prepared without quenching.⁹ The batch *B* crystals were doped with 1% Sr atoms (9290 ppm). Critical current density values were determined by magnetic hysteresis measurements for both types of crystals. A magnetic field was applied parallel to the *c* axis, and the supercurrent parallel to the *ab* plane was determined. The j_c values for the batch *A* and *B* specimens presented in Table I are assumed to be representative examples for each of the two types of crystals. The crystals described above were subsequently prepared for electron microscopic investigation, mainly by the powdering method. Small pieces of these crystals were crushed in an agate mortar and then transferred in water-free alcohol onto a copper grid covered with a holey carbon foil. A transmission electron microscope, Philips CM30ST (300 kV, spherical aberration constant $C_s = 1.1$ mm) was used for the HRTEM images together with selected area electron diffraction.

Figures 1(a) and 1(b) present HRTEM [001] micrographs in two different magnifications obtained from a crystal fragment of batch *A*, in which twin lamellae are a prominent microstructural feature. In this figure, a small-scale contrast feature, consisting of either bright or dark dots arranged in a rectangular cell, corresponds to the projected fundamental units of the perovskite cell in the $\text{YBa}_2\text{Cu}_3\text{O}_{7-\delta}$ crystal structure. In $\text{YBa}_2\text{Cu}_3\text{O}_{7-\delta}$, the cations Y and Ba, are chiefly responsible for the HRTEM contrast. Figure 1(c) is a Fourier-filtered image obtained from the (100) and (010) re-

TABLE I. Data on the synthesis and composition of batch *A* and *B* crystals used in this study. T_c , j_c , and B_{irr} denote critical temperature, critical current density, and irreversibility field, respectively. The peak field of batch *B* is 1 T.

Sample batch	Batch <i>A</i> (low j_c)	Batch <i>B</i> (high j_c)
Preparation	starting with 1 mol% Y_2O_3 , 26 mol% BaCO_3 , 72 mol% CuO	starting with 1 mol% Y_2O_3 , 26 mol% BaO doped with Sr, 72 mol% CuO (approx. 9290 ppm Sr)
	990 °C→939.1 °C:−0.6 °C/h →quenching	980 °C→940.6 °C:−0.5 °C/h →934.1 °C:−0.3 °C/h →slow cooling
Oxidation process	600 °C/50 h	590 °C/20 h
	→560 °C/100 h	→550 °C/100 h
	→500 °C/100 h	→500 °C/100 h
	→470 °C/100 h	→465 °C/100 h
	→450 °C/150 h	→445 °C/50 h
	→380 °C/140 h	→400 °C/70 h
T_c [K]	90.0	89.5
j_c (1 T, 77 K) [A/cm^2]	900	75 000
Peak effect	No	Yes ($B=1$ T)
B_{irr} (77 K) [T]	7	5

flections in the region corresponding to Fig. 1(b). The Fourier-filtered image was made by a circular mask with an apparent radius of $\sim \frac{1}{4}a^*$. The set of lattice planes along the [100] (or [010]) direction is slightly bent exactly at the twin boundary; however, they continue without interruption into the adjacent domains. This feature is typical for the usual, coherent twin boundaries, which are commonly observed in $\text{YBa}_2\text{Cu}_3\text{O}_{7-\delta}$ crystals.

Figure 2(a) is a HRTEM [001] image in intermediate magnification obtained from a batch *B* crystal. This image contains twin lamellae with horizontal boundaries marked by arrows. The contrast arising from this lamella is a typical microstructural feature in batch *B* crystals and is rather different from the contrast of the twin lamellae typically found in batch *A* crystals. This is evident from a comparison of Fig. 2(a) with Fig. 1(a) (notice that both images are in the same magnification). The contrast of every twin boundary in this crystal appears as a broad band of dark contrast and, moreover, the contrast consists of a sequence of many small dark patches, a few of which are marked by vertical white arrows. These dark patches in Fig. 2(a) are considered here to be associated with inhomogeneities of the strain field adjacent to the twin boundaries. In order to recognize the lattice distortions at the twin boundaries more clearly, computer-aided image processing was applied to the (100)-lattice plane, using Fourier filtering by a circular mask with an apparent radius of $\sim \frac{1}{4}a^*$. The result is shown in Fig. 2(c). This image allows us to clearly recognize the mode of continuation of the [100] lattice at the twin boundary: The lattice planes abruptly change their orientation, and in certain places, e.g., in the area enclosed by an oval in Fig. 2(c), a small lateral displacement along the boundary can be observed. This ob-

servation was made several times for many different areas, and this confirmed that the displacement occurs in all crystals of batch *B*, while it is rare in batch *A* crystals. We conjecture that this characteristic microstructure with its regular distribution^{4,5} may be the consequence of the Sr doping, whereby the Sr originates from the BaO material used in the synthesis (see Table I).

Zhu and Suenaga¹⁰ found twinning steps associated with a [100]-lattice displacement in $\text{YBa}_2\text{Cu}_3\text{O}_{7-\delta}$ crystals, and proposed that dislocations at the twin boundaries were the essential cause for a translational shift of [100]-lattice planes along the twin boundaries, attributing it to oxygen disorder in the boundary region. By contrast, the local structure of the twin interface of the present batch *B* crystals differs from that described in the previous studies mentioned above: The twin boundary contrast in batch *B* crystals more frequently indicates a local strain field, which causes lattice distortions near these boundaries, while the interfaces observed by Zhu *et al.* do not involve any strong distortion of the atomic structure.

This characteristic feature of the twin boundary interface may be correlated with the Sr doping (average Sr content 9290 ppm), since it was only very rarely found in the batch *A* crystals that did not contain any Sr. This allows the tentative conclusion that the lattice distortion along the twin boundary results from Sr atoms located in the vicinity of the twin boundary planes: These Sr atoms substitute for certain cations and may form clusters in the interstitial regions. A previous study¹¹ by neutron-scattering measurements combined with Rietveld refinement indicated that Sr atoms preferentially replace Ba atoms in the structure. Assuming that Sr^{2+} dominantly substitutes for Ba^{2+} , this substitution leads to a

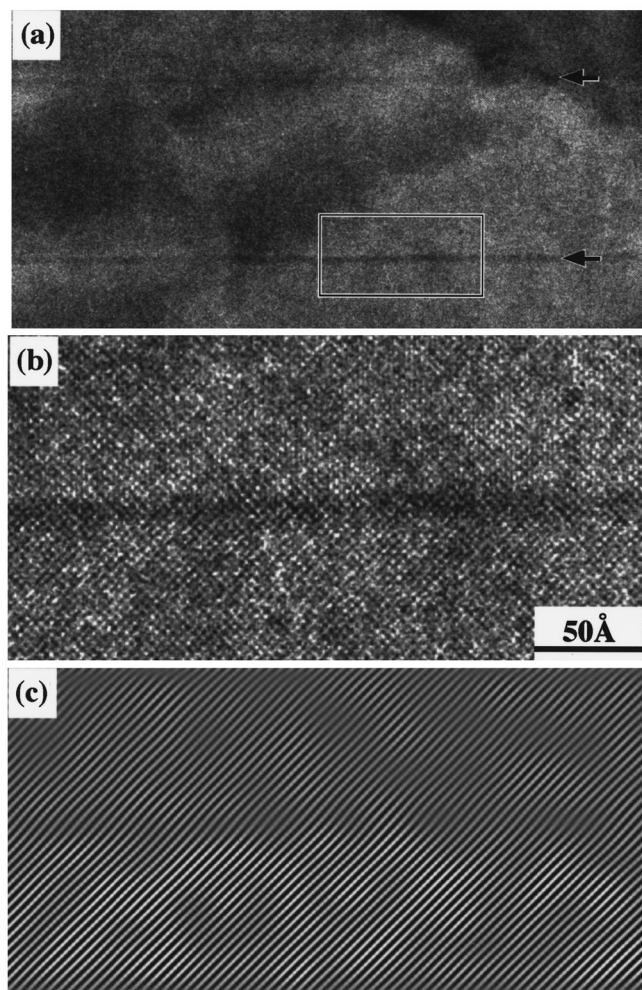


FIG. 1. HRTEM [001] image and the corresponding Fourier-filtered image obtained from a batch *A* crystal. (a) The image in intermediate magnification; (b) portion of (a) in high magnification. This area is marked by a rectangle in (a). The narrow strip of dark contrast recognized in the center corresponds to a region containing a twin boundary; (c) the corresponding Fourier-filtered image for [100]-lattice planes obtained from a region marked by a rectangle in Fig. 1(a). The image was made by selecting the (100) and (010) intensities from the Fourier-transformed image using a circular mask of approximate radius $\frac{1}{4} a^*$. Note that the lattice planes continue coherently across the twin domain.

substantial contraction of the unit cell, since the ionic radius of Sr^{2+} is considerably smaller than that of Ba^{2+} . Such a situation can lead to the contrast phenomena observed in the HRTEM images, i.e., that the crystal lattice is severely distorted near the twin boundaries and that this distortion involves translational displacements of the [100]-atom rows. The formation of Sr clusters in the interstitial regions may have the same effect as well. In order to obtain information on the effects of different contents of Sr, additional observations on twin textures were made in another type of crystal containing larger amounts of Sr (approx. 4 at. %). It was found that the twin texture characterized by local strain fields along the twin boundaries could only form in specimens containing a very small amount of Sr, e.g., 1%.

It is well known from recent work^{2,3} that “clean” twins do not cause strong flux pinning. In order to enhance j_c ,

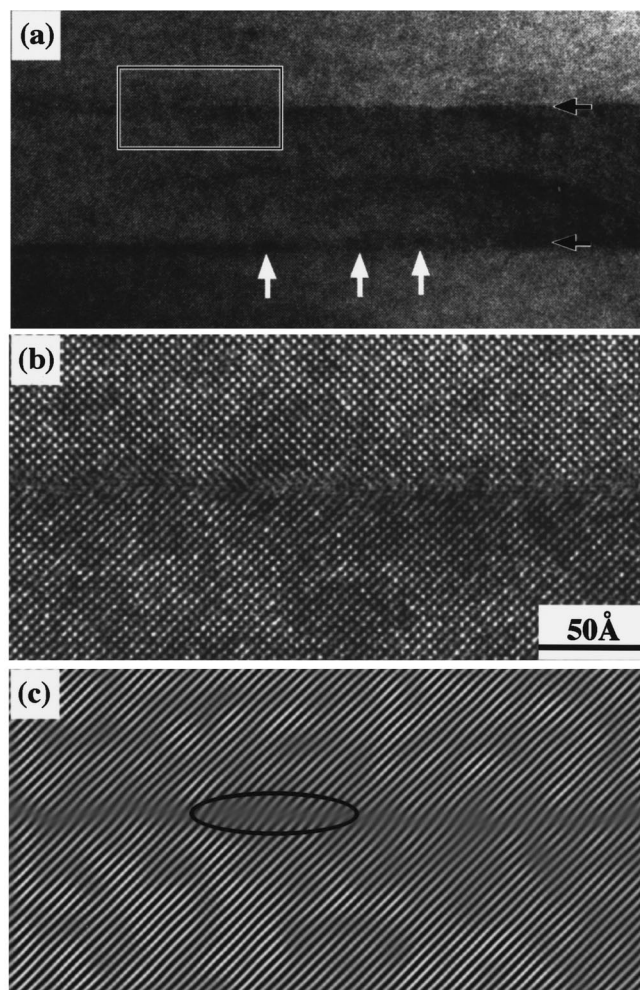


FIG. 2. HRTEM [001] image and the corresponding Fourier-filtered image obtained from a batch *B* crystal. (a) The image in intermediate magnification and (b) an enlarged HRTEM image from a region enclosed by a rectangle in (a). (c) The corresponding Fourier-filtered image for [100]-lattice planes obtained from a region marked by a rectangle in Fig. 1(a). The image was made by selecting the (100) and (010) intensities from the Fourier-transformed image using a circular mask of radius $\sim \frac{1}{4} a^*$. In the area enclosed by an oval, the lattice planes are seen to be discontinuous when they pass over the twin boundary.

additional defects have to be introduced. The most pronounced increase in pinning, the so-called fishtail or peak effect of $j_c(B)$, is created by pointlike defects or defect clusters, e.g., clusters of oxygen vacancies^{3,12} or dopants. There is experimental evidence from the present results that the Sr content of the batch *B* crystals results in isotropically distributed Sr clusters surrounded by local strain fields. This defect structure is responsible for the peak effect, i.e., the pronounced maximum of j_c at the peak field B_{peak} around 1 T. This is observed in batch *B*, but not in batch *A* crystals.³ The Sr clusters become visible in the TEM investigation as local strain fields adjacent to the twin boundaries, whereas homogeneously distributed Sr clusters in the bulk have no similar effect on the contrast of the HRTEM images. In the Sr-free, well-oxygenated and (also) twinned batch *A* crystals, the twin boundaries are intact and do not show distortions. A comparison of batch *A* and *B* crystals in Table I demonstrates

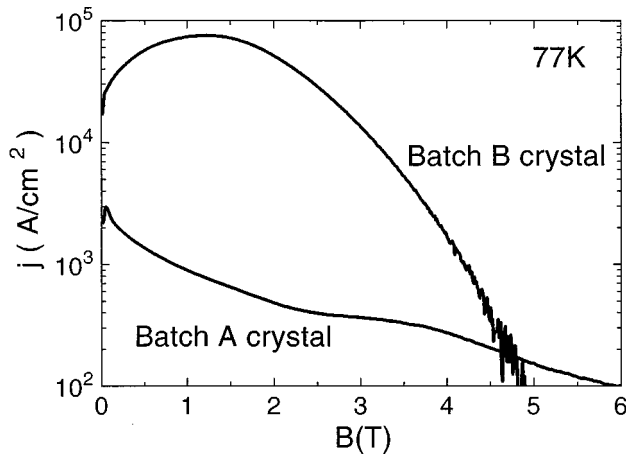


FIG. 3. Diagrams of j_c vs B for batch A and batch B crystals which were determined from measurements of magnetic hysteresis at 77 K. The geometric arrangement was chosen so that a magnetic field was applied along the c axis, while the supercurrent flowed within the ab plane.

the increase of j_c by a factor of approximately 80 at the peak field around 1 T due to Sr-induced strain field clusters.

The influence of twins on j_c becomes visible for the field orientation $\mathbf{B} \parallel c \parallel$ twin planes, and below the $j_c(B)$ peak, e.g., at $B=0.5$ T, even if it is not the dominant pinning mechanism. Angle-dependent measurements of the magnetic moment of batch B crystals reveal that the difference in j_c between the two field orientations outside and inside the trapping range of twins is less than 10%.³ In the latter case ($\mathbf{B} \parallel c \pm 15^\circ$), the twins act as planar pinning centers. This demonstrates that the twin structure in batch B crystals has only a minor influence on j_c , and is therefore not at all responsible for the peak effect. In addition, the fact that the influence of the twins on j_c is only small shows that an isotropic defect structure is the cause of the peak in the j_c values, i.e., the observed Sr clusters mentioned above. The twin density in batch B is about three times larger than in batch A crystals.⁵ This difference alone cannot account for the j_c increase by a factor of 80 compared to the j_c of batch A crystals. This finding also corroborates our conclusion that isotropically distributed Sr clusters, whose contrast is observed by TEM at the twin boundaries, are responsible for the peak effect, rather than the twin structures. The pronounced difference between the current density j_c of batch A and batch B is shown in Fig. 3. It demonstrates the continu-

ous decrease in j_c with rising magnetic field for the batch A crystal, in contrast to the observed peak of the current density for the Sr-doped batch B crystal. The significant increase in pinning is shown here to be caused by *isotropically* distributed Sr clusters, which is due to distortion of these boundaries. A detailed discussion of the interplay between pinning by clusters and twin boundaries is given in Ref. 3.

It should be noted that the batch B crystals have a higher level of j_c values than the batch A crystals, but that its irreversibility field (B_{irr}) is considerably lower than in batch A crystals. Theories of the vortex state in superconductor oxides predict^{13,14} that correlated defects such as twin boundaries as well as columnar defects artificially nucleated by ion irradiation allow for a characteristic vortex state, i.e., a Bose-glass state below the melting transition line in the magnetic phase diagram, and that this results in a prominent enhancement of the irreversibility field in the vicinity of $\mathbf{B} \parallel c$. It was also suggested³ that the variation in the twin texture significantly changed the B_{irr} values. The twin boundaries of batch B crystals, which are decorated by the strain fields, are not atomically planar. This lowers the efficiency of *correlated* pinning of the twin boundaries, and may be the reason for batch B crystals having considerably lower B_{irr} values than batch A crystals.

In conclusion, our TEM observations, combined with computer image processing, allow us to differentiate the twin textures of crystals of batch B from those of batch A. The present results therefore lead to the conclusion that the twin boundaries of batch B crystals are decorated with localized strain fields, having an extension of 20–50 Å, in which the crystallographic lattice is significantly distorted. The Fourier filtering executed by computer confirms the presence of lattice distortions. We ascribe this characteristic twin texture to the presence of a specific, critical trace amount of Sr atoms (approx. 1 at. %) in batch B crystals in a probably homogeneous distribution. We propose that strain field clusters are effective flux pinning centers in Sr-doped $\text{YBa}_2\text{Cu}_3\text{O}_{7-\delta}$ crystals causing the peak effect in $j_c(B)$.

The present work has profited much from discussions with Professor K. Hiraga, to whom we are very grateful. We would also like to acknowledge technical assistance in electron microscopic work by R. Wessicken, P. Wägli, and A. Sigg. We are indebted to D. Grindatto, S. Ritsch, and T. Ohsumi for efficient help with the computer work. This research has been supported by the Swiss National Foundation, Grant No. 20-40403.94/1, for which we are also grateful.

*Present address: Department of Materials Engineering and Applied Chemistry, Akita University, Akita City, 010-8502, Japan.

¹Z. L. Wang, A. Goyal, and D. M. Kroeger, *Phys. Rev. B* **47**, 5373 (1993).

²H. Fujimoto, T. Taguchi, M. Murakami, and K. Koshizuka, *Physica C* **211**, 393 (1993).

³H. Küpfer, A. A. Zhukov, A. Will, W. Jahn, R. Meier-Hirmer, T. Wolf, V. I. Voronkova, M. Kläser, and K. Saito, *Phys. Rev. B* **54**, 644 (1996).

⁴Y. Xu, M. Suenaga, J. Taftø, R. L. Sabatini, A. R. Moodenbaugh, and P. Zolliker, *Phys. Rev. B* **39**, 6667 (1989).

⁵K. Saito, H.-U. Nissen, T. Wolf, W. Schauer, and C. Beeli,

Czech. J. Phys. **46**, 1545 (1996).

⁶Y. Zhu, M. Suenaga, and Y. Xu, *Philos. Mag. Lett.* **60**, 51 (1989).

⁷Y. Zhu, M. Suenaga, Y. Xu, R. L. Sabatini, and A. R. Moodenbaugh, *Appl. Phys. Lett.* **54**, 374 (1989).

⁸Y. Zhu, M. Suenaga, J. Taftø, and D. O. Welch, *Phys. Rev. B* **44**, 2871 (1991).

⁹T. Wolf, W. Goldacker, B. Obst, G. Roth, and R. Flükiger, *J. Cryst. Growth* **96**, 1010 (1989).

¹⁰Y. Zhu and M. Suenaga, *Philos. Mag. A* **66**, 457 (1992).

¹¹B. W. Veal, W. K. Kwok, A. Umezawa, G. W. Crabtree, J. D. Jorgensen, J. W. Downey, L. J. Nowicki, A. W. Mitchell, A. P.

- Paulikas, and C. H. Sowers, *Appl. Phys. Lett.* **51**, 27 (1987); **51**, 279 (1987).
- ¹²A. Erb, J.-Y. Genoud, F. Marti, M. Däumling, E. Walker, and R. Flükiger, *J. Low Temp. Phys.* **105**, 1023 (1996).
- ¹³D. R. Nelson and V. M. Vinokur, *Phys. Rev. Lett.* **68**, 2398 (1992).
- ¹⁴G. Blatter, M. V. Feigel'man, V. B. Geshkenbein, A. I. Larkin, and V. M. Vinokur, *Rev. Mod. Phys.* **105**, 1023 (1996).